Strong Inhibition of Singlet Oxygen Sensitization in Pyridylferrocene−Fluorinated Zinc Porphyrin Supramolecular Complexes

Yukiyasu Kashiwagi,[†] Hiroshi Imahori,*[,‡] Yasuyuki Araki,[§] Osamu Ito,*[,§] Koji Yamada,[||] Yoshiteru Sakata,[||] and Shunichi Fukuzumi*[,†]

Department of Material and Life Science, Graduate School of Engineering, Osaka University, CREST, Japan Science and Technology Corporation (JST), Suita, Osaka 565-0871, Japan, Department of Molecular Engineering, Graduate School of Engineering, Kyoto University, PRESTO, JST, Sakyo-ku, Kyoto 606-8501, Japan, Fukui Institute for Fundamental Chemistry, Kyoto University, 34-4, Takano-Nishihiraki-cho, Sakyo-ku, Kyoto 606-8103, Japan, Institute for Multidisciplinary Research for Advanced Materials, Tohoku University, CREST, JST, Katahira, Aoba-ku, Sendai 980-8577, Japan, and The Institute of Scientific and Industrial Research, Osaka University, Ibaraki, Osaka 567-0047, Japan

Received: April 8, 2003

A supramolecular pyridylferrocene (PyFc)−fluorinated zinc porphyrin (ZnTFPP) dyad system was developed, and its photodynamics was investigated in dichloromethane and acetonitrile. The nitrogen of PyFc coordinates to the metal center of zinc porphyrin to form a supramolecular donor−acceptor complex. Formation of the pyridylferrocene−zinc porphyrin supramolecule was probed by ^{1}H NMR and UV−vis spectroscopy. The one-electron reduction potential of ZnTFPP in dichloromethane is shifted to a negative direction by 0.08 V due to formation of the supramolecular complex with PyFc. The binding constant of ZnTFPP$^{\bullet-}$ with PyFc in the supramolecular complex determined from the potential shift is much smaller than the binding constant of the neutral form, ZnTFPP. The fluorescence of ZnTFPP is strongly quenched by electron transfer from PyFc to the singlet excited state (^{1}ZnTFPP*) in the supramolecular complex of ZnTFPP with PyFc. The lifetime of ^{1}ZnTFPP* is also shortened significantly in the supramolecular complex. No transient absorption spectrum due to the charge-separated state (ZnTFPP$^{\bullet-}$−PyFc$^+$) or the triplet excited state (^{3}ZnTFPP*−PyFc) was detected even at the picosecond time scale due to the ultrafast back electron transfer from ZnTFPP$^{\bullet-}$ to PyFc$^+$ to yield the ground state supramolecular complex rather than the triplet excited state. This leads to strong inhibition of singlet oxygen sensitization of the zinc porphyrin by formation of the supramolecular complex.

Introduction

Porphyrin-based photosensitizers have been the subject of enormous interest due to their potential use in photodynamic therapy (PDT).[1] The photosensitizing agent is photoexcited by visible light to the singlet excited state which is efficiently converted by intersystem crossing to the triplet excited state, followed by energy transfer to molecular oxygen to produce the singlet oxygen which is a putative cytotoxic agent.[1,2] On the other hand, porphyrins with highly delocalized π systems are suitable for efficient electron transfer, because the uptake or release of electrons results in minimal structural change upon electron transfer.[3] Rich redox properties render porphyrins and metalloporphyrins as essential components in important biological electron transport systems including photosynthesis and respiration.[4] Thus, continuous efforts have been devoted to study electron transfer reactions of covalently linked electron donor−acceptor ensembles containing porphyrins and metalloporphyrins, mimicking the biological electron transfer systems.[5−9] An increasing number of noncovalently linked supramolecular assemblies containing porphyrins and metalloporphyrins have also been developed extensively.[10−16] The main objective of studies on covalently or noncovalently linked donor−acceptor ensembles has so far been focused on creating long-lived charge-separated (CS) states to be utilized for light energy conversion purposes.[5−16] Such CS states, which are highly reactive, can also act as putative cytotoxic agents. When the triplet excited states of porphyrins are lower in energy as compared to the CS states of donor−acceptor dyads containing porphyrins, the back electron transfer from the charge-separated states normally results in formation of either the ground state or the triplet excited state of porphyrins, which leads to generation of singlet oxygen.[17,18] In general, the larger the reorganization energy (λ) of electron transfer, the slower the forward photoinduced electron transfer of the singlet excited state of porphyrins in the Marcus normal region[19] leading to the higher triplet yield of porphyrins because of the competing intersystem crossing to the triplet state.[7] Conversely, the smaller the λ value of electron transfer, the faster the forward photoinduced electron transfer but the slower the back electron transfer to the ground state in the Marcus inverted region. When the triplet excited state is lower in energy than the radical ion pair, the back electron transfer to the triplet excited state in the Marcus normal region becomes faster than the back electron transfer to the ground state in the Marcus inverted region. In each case, the

* To whom correspondence should be addressed. E-mail: imahori@scl.kyoto-u.ac.jp; fukuzumi@ap.chem.eng.osaka-u.ac.jp; ito@tagen.tohoku.ac.jp.

[†] Department of Material and Life Science, Graduate School of Engineering, Osaka University, CREST, Japan Science and Technology Corporation (JST).

[‡] Department of Molecular Engineering, Graduate School of Engineering, Kyoto University, PRESTO, JST, and Fukui Institute for Fundamental Chemistry, Kyoto University.

[§] Institute for Multidisciplinary Research for Advanced Materials, Tohoku University, CREST, JST.

[||] The Institute of Scientific and Industrial Research, Osaka University.

10.1021/jp034920q CCC: $25.00
Published on Web 06/28/2003

CHART 1

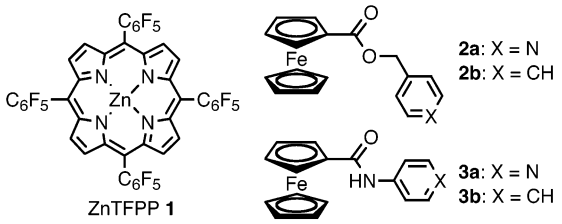

formation of the triplet excited state of porphyrins leads to generation of singlet oxygen in the presence of oxygen via efficient energy transfer from the triplet excited state to oxygen.[17] The efficient generation of singlet oxygen is of primary importance to develop photosensitizers for their use in PDT. It is also important to find a way to inhibit generation of singlet oxygen whenever it is desired after PDT, since the exposure to light needs to be prohibited for a long time. Carotenoid pigments are known to quench the chlorophyll singlet excited state both in vivo and in vitro,[20] preventing the chlorophyll- and porphyrin-sensitized formation of singlet oxygen by intercepting the triplet states via photoinduced electron transfer.[21−23] In this context, carotenoid−porphyrin linked systems have been extensively studied to limit damage in tumor imaging applications related to PDT.[24,25] However, there has so far been no report on a supramolecular porphyrin system which inhibits the generation of singlet oxygen in sensitization of porphyrins.

Such a supramolecular porphyrin system to inhibit generation of singlet oxygen would be attained provided that one can design a system in which the λ value is small enough to achieve efficient forward photoinduced electron transfer of the singlet excited state of porphyrins but the λ value becomes larger for the back electron transfer from the radical ion pair to facilitate the back electron transfer to the ground state rather than to the triplet state. In principle, such a drastic change in the λ value between the forward electron transfer and back electron transfer is possible, since the coordination binding constant, which is related to the binding distance, is known to be changed drastically depending on the oxidation state of metalloporphyrins[26] and the λ value increases with increasing the donor and acceptor binding distance.[17] However, the effects of the change in the binding constants upon electron transfer in supramolecular complexes have yet to be examined.

We report herein a novel supramolecular system consisting of pyridylferrocenes and a fluorinated zinc porphyrin (Chart 1), in which the generation of singlet oxygen in sensitization of the zinc porphyrin is strongly inhibited by formation of the supramolecular complex. The fluorinated zinc porphyrin is used to facilitate the photoinduced electron transfer from the ferrocene moiety to the zinc porphyrin moiety by the electron-withdrawing effect of fluoro-substituents. The change in the binding constant of the supramolecular complex depending on the oxidation state of zinc porphyrins is investigated by spectroscopic and electrochemical measurements. The inhibition mechanism is revealed from a detailed study on the electrochemical and photophysical properties of the supramolecular complexes.

Experimental Section

General. Melting points were recorded on a Yanagimoto micromelting point apparatus and not corrected. ^{1}H NMR spectra were measured on a JEOL EX-270 (270 MHz) or a JEOL JMN-AL300 (300 MHz). Fast atom bombardment mass spectra (FABMS) were obtained on a JEOL JMS-DX300. IR spectra were measured on a Perkin-Elmer FT-IR 2000 spectrophotometer as KBr disks. Elemental analyses were performed on a Perkin-Elmer model 240C elemental analyzer.

Materials. All solvents and chemicals were of reagent grade quality, obtained commercially and used without further purification unless otherwise noted (vide infra). Tetrabutylammonium perchlorate (TBAP) used as a supporting electrolyte in dichloromethane and acetonitrile for the electrochemical measurements was obtained from Tokyo Kasei Organic Chemicals. Tetrahexylammonium perchlorate (THAP) used as a supporting electrolyte in benzene was prepared by the addition of $NaClO_4$ to the tetrahexylammonium bromide in acetone, followed by recrystallization from acetone. Dichloromethane (CH_2Cl_2) was purchased from Wako Pure Chemical Ind., Ltd., and purified by successive distillation over calcium hydride. Thin-layer chromatography (TLC) and flash column chromatography were performed with an Art. 5554 DC-Alufolien Kieselgel 60 F254 (Merck) and a Fujisilicia BW300, respectively.

Zn(II) Complex of 5,10,15,20-Tetrakis(pentafluorophenyl)porphyrin (1). A solution of pyrrole (0.70 mL, 10 mmol) and pentafluorobenzaldehyde (1.28 mL, 10 mmol) in CH_2Cl_2 (400 mL) was degassed by bubbling with nitrogen for 30 min. The reaction vessel was shielded from ambient light. Then, boron trifluoride diethyl etherate (0.30 mL, 3.0 mmol) was added in one portion. The solution was refluxed for 4 h under a nitrogen atmosphere. To the reaction mixture, *p*-chloranil (1.85 g, 6.4 mmol) was added and refluxed for 12 h. After cooling, the reaction mixture was washed with a saturated $NaHCO_3$ aqueous solution and water. After standing over anhydrous Na_2SO_4, the organic extract was concentrated to dryness. The organic layer was evaporated. Flash column chromatography on silica gel with $CHCl_3$−hexane (2:3) as the eluent gave a pale red solid. A saturated methanol solution of $Zn(OAc)_2$ (5.0 mL) was added to a $CHCl_3$ solution of the pale red solid (50 mL) and refluxed for 10 h. After cooling, the reaction mixture was washed with water twice and dried over anhydrous Na_2SO_4, and the solvent was evaporated. Column chromatography on silica gel with $CHCl_3$ as an eluent and subsequent reprecipitation from $CHCl_3$−hexane gave **1** as a pink solid (181 mg, 0.175 mmol, 7% yield). ^{1}H NMR (270 MHz, $CDCl_3$) δ 9.01 (8H, s); FABMS *m*/*z* 1036 (M^+).

4-Pyridylmethyl Ferrocenylcarboxylate (2a). Oxalyl chloride (1.0 mL, 12 mmol) was added to a stirred solution of ferrocenylcarboxylic acid (500 mg, 2.17 mmol) in dry CH_2Cl_2 (20 mL) and pyridine (0.01 mL). The resulting solution was stirred for 14 h at room temperature and refluxed for 5 h. Excess oxalyl chloride and solvents were removed under reduced pressure, and the residue was redissolved in dry CH_2Cl_2 (20 mL). A CH_2Cl_2 solution of 4-pyridinecarbinol (2.20 g, 20.2 mmol) was added to the resulting solution, and the solution was stirred for 12 h. The reaction mixture was washed with a saturated $NaHCO_3$ aqueous solution and water. The organic layer was dried over anhydrous Na_2SO_4, and then the solvent was evaporated. The residue was purified by silica gel column chromatography ($CHCl_3$/NEt_3 = 19/1 (v/v) as eluent) to afford **2a** as a orange solid (314 mg, 0.977 mol, 45% yield). mp 83.5−84.5 °C (dec); ^{1}H NMR (270 MHz, $CDCl_3$) δ 8.64 (d, J = 6 Hz, 2H), 7.35 (d, J = 6 Hz, 2H), 5.28 (s, 2H), 4.87 (t, J = 2 Hz, 2H), 4.45 (t, J = 2 Hz, 2H), 4.18 (s, 5H); FT-IR (KBr) 1704 cm^{-1} ($\nu_{C=O}$); UV−vis (CH_2Cl_2) λ_{max} (log ϵ) = 447.2 (1.41), 311.6 (2.07), 255.1 (2.87); EI MS *m*/*z* 321 (M^+). Anal. Calcd for $C_{17}H_{15}FeNO_2$: C, 63.58; H, 4.71; N, 4.36. Found: C, 63.32; H, 4.47; N, 4.15.

Benzyl ferrocenylcarboxylate (**2b**), ferrocenylamido-4-pyridine (**3a**), and ferrocenylamido-4-benzene (**3b**) were also synthesized by acid chloride-mediated condensation and characterized by ^{1}H NMR, UV−vis, FABMS spectra, and elemental analysis (see Supporting Information S1 and S2).

Spectral Measurements. Time-resolved fluorescence spectra were measured by a single-photon counting method using a second harmonic generation (SHG, 410 nm) of a Ti:sapphire laser (Spectra-Physics, Tsunami 3950-L2S, 1.5 ps full width at half-maximum (fwhm)) and a streakscope (Hamamatsu Photonics, C4334-01) equipped with a polychromator (Acton Research, SpectraPro 150) as an excitation source and a detector, respectively.[18]

The picosecond laser flash photolysis was carried out using a second harmonic generation (SHG, 388 nm) of a mode-locked Ti:sapphire laser (Clark-MXR CPA-2001) as an exciting source. The excitation laser was depolarized. A white continuum pulse generated by focusing the fundamental of a Nd:sapphire laser on a H_2O cell was used as monitoring light. A pump−probe system with a dual MOS detector (Hamamatsu Photonics, C6140) equipped with a polychromator (Acton Research, SpectraPro 150) was applied for the measurements of the transient absorption spectra.[18]

Nanosecond transient absorption measurements were carried out using an OPO laser (Continuum, Surelite OPO, fwhm 4 ns, 555 nm) pumped by a Nd:YAG laser (Continuum, SLII-10, 4−6 ns fwhm) as an excitation source. Photoinduced events in nanosecond time regions were monitored by using a continuous Xe-lamp (150 W) and an Si-APD photodiode (Hamamatsu 2949) as a probe light and a detector, respectively. The output from the photodiodes was recorded with a digitizing oscilloscope (HP, 54810A, 500 MHz). All the samples in a quartz cell (1 × 1 cm) were deaerated by bubbling argon through the solution for 15 min.[18]

Steady-state absorption spectra were measured on a Hewlett-Packard 8452A diode array spectrophotometer at 298 K. Steady-state fluorescence spectra were measured on a Perkin-Elmer LS50B fluorescence spectrophotometer. Quenching experiments of the fluorescence of ZnTFPP−PyFc complexes were performed on a SHIMADZU spectrofluorophotometer (RF-5000PC). The excitation wavelength of ZnTFPP and ZnTFPP−PyFc complexes was 555 nm in deaerated CH_2Cl_2 and CH_3CN. The solutions were deaerated by argon purging for 7 min prior to the measurements.

Electrochemical Measurements. Cyclic voltammetry measurements were performed at 298 K on a BAS 100W electrochemical analyzer in deaerated CH_2Cl_2 containing 0.1 M TBAP as a supporting electrolyte. A conventional three-electrode cell was used with a platinum button working electrode and a platinum wire as the counter electrode. The measured potentials were recorded with respect to the $Ag/AgNO_3$ reference electrode. All potentials (vs Ag/Ag^+) were converted to values versus saturated calomel electrode (SCE) by adding 0.29 V.[27] The $E_{1/2}$ value of ferrocene used as a standard is 0.37 V versus SCE in CH_2Cl_2 under the present experimental conditions. All electrochemical measurements were carried out under an atmospheric pressure of argon.

Results and Discussion

Synthesis. Tetrakis(pentafluorophenyl)porphyrinatozinc (**1**, ZnTFPP) was prepared according to Lindsey's method.[28] Pyridylferrocenes (**2a** and **3a**, PyFc) and their reference compounds **2b** and **3b** were also synthesized by acid chloride-mediated condensation as shown in Scheme 1.[29] These molecules were well-characterized by ^{1}H NMR, UV−vis, FABMS spectra, and elemental analysis (see Experimental Section).

SCHEME 1

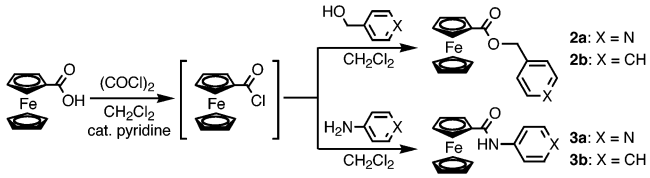

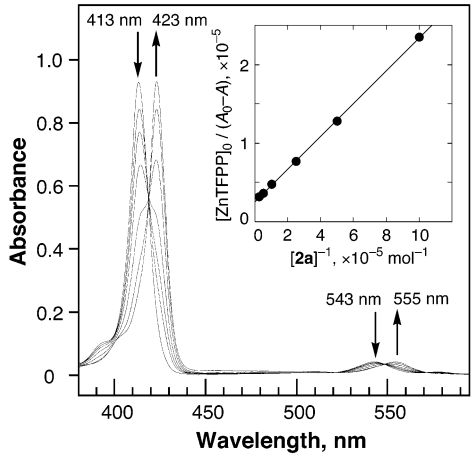

Figure 1. UV−visible spectra of ZnTFPP (1.0×10^{-6} M) in the presence of various concentrations of **2a** (1.0×10^{-6} to 2.0×10^{-5} M) in CH_2Cl_2. Inset: Plot of $[ZnTFPP]_0/(A_0 - A)$ vs $[\mathbf{2a}]^{-1}$ at 413 nm.

Formation of a ZnTFPP−PyFc Complex. The UV−vis spectra of ZnTFPP in CH_2Cl_2 at 298 K are changed upon addition of **2a** as shown in Figure 1, where the Soret and Q-bands are red-shifted with isosbestic points. The absorbance change exhibits a saturation behavior with increasing **2a** concentration. This indicates that **2a** forms a 1:1 complex with ZnTFPP (eq 1). Such nitrogenous bases readily bind to zinc

$$\mathrm{ZnTFPP} + \mathrm{PyFc} \overset{K}{\rightleftharpoons} (\mathrm{ZnTFPP}\cdots\mathrm{PyFc}) \qquad (1)$$

porphyrins with a 1:1 stoichiometry.[30,31] According to eq 1, the absorbance change is given by eq 2,[32] which predicts a linear correlation between $[ZnTFPP]_0/(A_0 - A)$ and $[PyFc]^{-1}$, where

$$[\mathrm{ZnTFPP}]_0/(A_0 - A) = 1/(\epsilon_c - \epsilon_p) + (K[\mathrm{PyFc}](\epsilon_c - \epsilon_p))^{-1} \qquad (2)$$

A_0 and A are the absorbance of ZnTFPP at 413 nm in the absence and presence of PyFc, and ϵ_p and ϵ_c are the molar absorption coefficients of ZnTFPP at 413 nm in the absence and presence of PyFc, respectively. From a linear plot of $[ZnTFPP]_0/(A_0 - A)$ versus $[PyFc]^{-1}$ is determined the formation constant as 1.2×10^5 M^{-1} in CH_2Cl_2. The formation constants (K) were also determined for **2a** and **3a** in benzene, acetonitrile (CH_3CN) and CH_2Cl_2 as listed in Table 1.

The binding constant of the ZnTFPP−**3a** complex in CH_2Cl_2 is larger than that of the ZnTFPP−**2a** complex. This can be ascribed to the higher basicity of the pyridine moiety resulting from the electron-donating group at the 4-position. The binding constant of **2a** in CH_3CN is 1.9×10^3 M^{-1}, which is significantly smaller than the value in CH_2Cl_2 because of the competing coordination of CH_3CN. The smaller K value in benzene than in CH_2Cl_2 may be attributed to the π interaction with benzene.

TABLE 1: Binding Constants (K) of the ZnTFPP (1) Complexes with PyFc (2a and 3a), One-Electron Oxidation Potentials (E^0_{ox}) of PyFc, and Reduction Potentials (E^0_{red}) of the 1−Pyridine Complex at 298 K

	K, M^{-1} [a]		E^0_{ox} vs SCE, V		E^0_{red} vs SCE, V
solvent	**2a**	**3a**	**2a**	**3a**	**1**−pyridine
CH_2Cl_2	1.2×10^5	2.2×10^5	0.74[b]	0.73[b]	−1.03[b]
CH_3CN	1.9×10^3	8.3×10^3	0.63[b]	0.61[b]	−1.04[b]
C_6H_6	1.9×10^4	3.7×10^4	0.68[c]	0.67[c]	−0.97[c]

[a] The experimental error is ±10%. [b] In the presence of 0.1 M TBAP as supporting electrolyte. [c] In the presence of 0.1 M THAP as supporting electrolyte.

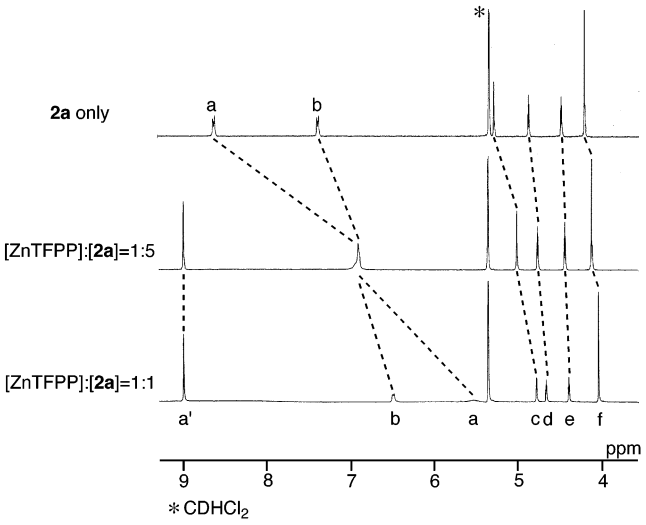

Figure 2. ^{1}H NMR spectra of **2a** in the presence of various concentrations of ZnTFPP in CD_2Cl_2. Peaks a and b are the protons in the pyridine ring, peak c is in the spacer CH_2, peaks d−f are in the ferrocene ring, and peak a′ is in the β-position of ZnTFPP.

The ^{1}H NMR signals of free **2a** exhibit upfield shifts upon complexation with ZnTFPP in CD_2Cl_2 as shown in Figure 2. The signals of the free **2a** and the complexed **2a** always coalesced into a single signal. This indicates that the complexation occurs faster than the NMR time scale. The large upfield shift of the pyridyl aromatic protons of **2a** (3.28 ppm) induced by the complexation is ascribed to the large porphyrin aromatic ring-current.[33] This clearly indicates that the pyridyl group of **2a** coordinates axially to the central zinc ion of ZnTFPP.

Change in the Binding Constant Depending on the Oxidation State. The change in the one-electron reduction potential of ZnTFPP by the supramolecular complex formation with **2a** was examined by cyclic voltammetry in CH_2Cl_2 containing 0.1 M TBAP. The one-electron reduction potential of ZnTFPP is shifted to a negative direction in the presence of **2a**. The potential shift increases with increasing **2a** concentration to reach the one-electron reduction potential of the ZnTFPP−**2a** complex as shown in Figure 3. The potential shift ($\Delta E_{1/2}$) is given by the Nernst equation (eq 3),

$$\Delta E_{1/2} = (2.3RT/F)\log(K/K^-) \quad (3)$$

where K^- is the binding constant of ZnTFPP$^{\bullet-}$ with **2a**. The K^- value is determined from the $\Delta E_{1/2}$ and the K value as 5.5×10^3 M^{-1}, which is much smaller than the K value (1.2×10^5 M^{-1}). Similarly, the K^- value of **3a** in CH_2Cl_2 was determined as 6.3×10^3 M^{-1} which is also much smaller than the corresponding K value (2.2×10^5 M^{-1}).[34] The much smaller K^- values as compared with the corresponding K values indicate that the binding in the ZnTFPP−**2a** complex becomes much weaker upon the one-electron reduction.

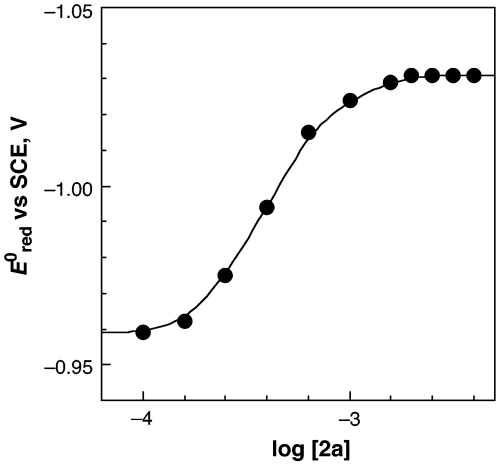

Figure 3. Dependence of the one-electron reduction potential of ZnTFPP (1.0×10^{-4} M) on the concentration of **2a** ($0-4.0 \times 10^{-3}$ M) in CH_2Cl_2 containing 0.1 M TBAP at 298 K. Scan rate = 100 mV/s.

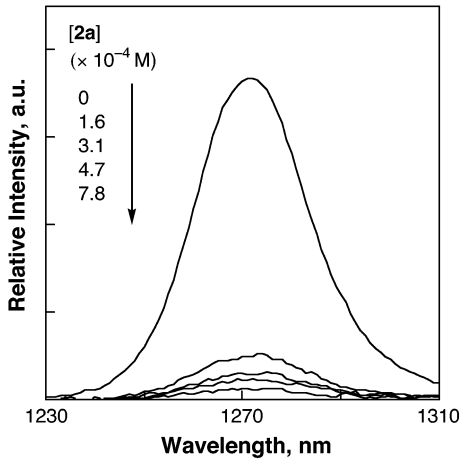

Figure 4. The phosphorescence spectra of singlet oxygen sensitized by irradiation of ZnTFPP (1.1×10^{-5} M) at 551 nm in the presence of various concentrations of **2a** in oxygen-saturated C_6D_6 at 298 K.

2a exhibits the reversible wave for the one-electron oxidation to the ferricenium cation ($PyFc^+$). The one-electron oxidation potentials of **2a** and **3a** are shifted cathodically by about 0.2 V as compared with those of the nonsubstituted ferrocene because of the electron-withdrawing carbonyl function. The one-electron oxidation potentials are also listed in Table 1.

Inhibition of Singlet Oxygen Sensitization by Supramolecular Complex Formation. Photoirradiation of ZnTFPP with light of λ = 551 nm in O_2-saturated benzene-d_6 results in generation of singlet oxygen which is detected by the $^1O_2$ phosphorescence at 1270 nm[35] as shown in Figure 4. Upon addition of **2a**, the $^1O_2$ phosphorescence intensity decreases significantly (Figure 4). The phosphorescence quantum yields (Φ) were determined using tetraphenylporphyrin (TPP) as a standard.[36] The Φ values are summarized in Table 2. The Φ value (75%) is drastically reduced to 2.3% in the presence of **2a** (7.8×10^{-4} M), where most ZnTFPP molecules form the complex with **2a** judging from the K value in benzene (Table 1).[37] In contrast, the Φ value is only slightly decreased to 52% when **2a** is replaced by **2b** which has no coordination site to ZnTFPP. The Φ value of the ZnTFPP−pyridine complex is 60%. Thus, singlet oxygen sensitization of ZnTFPP is strongly

TABLE 2: Relative Quantum Yields (Φ) of Singlet Oxygen Generated by Irradiation of ZnTFPP (1) in Oxygen-Saturated C_6D_6 at 298 K ([1] = 1.1 × 10^{-5} M, [2a] = [2b] = 7.8 × 10^{-4} M, [Pyridine] = 2.1 × 10^{-2} M)

compound	Φ,[a] %	compound	Φ,[a] %
TPP (standard)	62[b]	**1**-pyridine	60
1	75	**1**-pyridine + **2b**	52
1−**2a**	2.3		

[a] Excitation at λ = 551 nm, using TPP (Φ = 0.62 in C_6D_6) as standard. [b] Taken from ref 36.

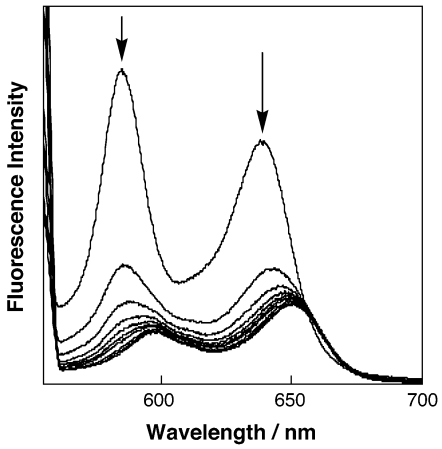

Figure 5. Fluorescence spectra of ZnTFPP (5.0 × 10^{-6} M) in the presence of various concentrations of **2a** (0−1.0 × 10^{-3} M) in deaerated benzene. The arrows indicate the direction of change.

inhibited by complexation with **2a**. To clarify the origin of such strong inhibition of singlet oxygen sensitization, the photophysical properties of the ZnTFPP−PyFc complex are examined in comparison with those of ZnTFPP (vide infra).

Photophysical Properties of the ZnTFPP−PyFc Complex. Photoexcitation of the Q-band of ZnTFPP at 555 nm in benzene results in fluorescence at λ_{max} = 585 and 638 nm as shown in Figure 5. Addition of **2a** to a benzene solution of ZnTFPP results in a significant change in the fluorescence spectrum of ZnTFPP. The fluorescence intensity of ZnTFPP decreases with increasing **2a** concentration and the fluorescence maxima are red-shifted to λ_{max} = 599 and 651 nm, when ZnTFPP is converted completely to the ZnTFPP−**2a** complex (Figure 5). When **2a** is replaced by **3a**, the fluorescence quenching of ZnTFPP by **3a** is much less efficient as compared with the case of **2a**, although the binding constant of the ZnTFPP−**3a** complex (3.7 × 10^4 M^{-1}) is larger than the binding constant of the ZnTFPP−**2a** complex (1.9 × 10^4 M^{-1}). The amide spacer of **3a** is rigid, whereas the ester spacer of **2a** is flexible. Such a flexibility of the spacer of **2a** enables formation of the ZnTFPP−**2a** complex in which the distance between the ferrocene and the porphyrin moiety is closer than the distance in the ZnTFPP−**3a** complex with the rigid spacer, resulting in the more efficient quenching in the ZnTFPP−**2a** complex. In the noncoordinative reference system, that is, the ZnTFPP−pyridine complex with **2b** or **3b**, however, the fluorescence of the ZnTFPP−pyridine complex is hardly quenched by the intermolecular reaction with **2b** or **3b**.

The fluorescence lifetimes of the ZnTFPP−PyFc complexes and the reference systems were determined using a single-photon counting method. The fluorescence of ZnTFPP in benzene exhibits a single-exponential decay with a lifetime of 1.4 ns. The fluorescence lifetime remains approximately the same when ZnTFPP forms a complex with pyridine (2.1 × 10^{-2} M) in benzene (1.6 ns). When **2a** is added to a benzene solution of

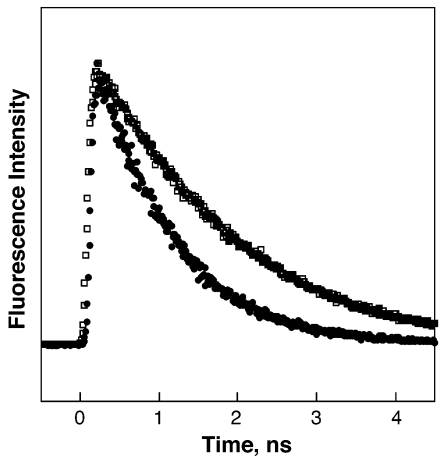

Figure 6. Fluorescence decay profiles of supramolecular complexes [ZnTFPP−**2a** complex (closed circle), ZnTFPP−pyridine complex (open square)] in deaerated benzene by excitation (555 nm) at emission wavelength = 600 nm. [ZnTFPP] = 1.0 × 10^{-5} M, [**2a**] = 1.0 × 10^{-3} M, [pyridine] = 2.1 × 10^{-2} M.

TABLE 3: Fluorescence Lifetimes (τ) and Quenching Rate Constants (k_q) of the ZnTFPP (1) and 1−PyFc Complexes at 298 K ([1] = 1.0 × 10^{-5} M, [2] = [3] = 1.0 × 10^{-3} M, [Pyridine] = 2.1 × 10^{-2} M)

	C_6H_6		CH_2Cl_2		CH_3CN	
	τ, ns	k_q, s^{-1}	τ, ns	k_q, s^{-1}	τ, ns	k_q, s^{-1}
1	1.4		1.4		1.6	
1−pyridine	1.6	6.3 × 10^8	1.4	7.1 × 10^8	1.5	6.7 × 10^8
1−**2a**	0.96	4.2 × 10^8	0.52	1.2 × 10^9	0.38	2.0 × 10^9
1−**3a**	1.5	4.2 × 10^7	1.3	5.5 × 10^7		
1-pyridine + **2b**	1.6	0	1.4	0	1.4	4.8 × 10^7
1-pyridine + **3b**	1.6	0	1.4	0		

ZnTFPP, the fluorescence decay consists of two lifetimes (1.6 and 0.96 ns). The shorter lifetime component increases with increasing **2a** concentration as shown in Figure 6. Under the conditions where all ZnTFPP molecules form the complex with **2a**, the fluorescence decay exhibits a single-exponential decay with the lifetime of 0.96 ns which corresponds to the fluorescence lifetime of the ZnTFPP−**2a** complex. In contrast to the case of the ZnTFPP−**2a** complex, the fluorescence lifetime of the ZnTFPP−**3a** complex (1.5 ns) is virtually the same as that of the ZnTFPP−pyridine complex (1.6 ns). This is consistent with the little quenching of the steady-state fluorescence in the ZnTFPP−**3a** complex due to the larger distance between ZnTFPP and **3a** as compared with the case of the ZnTFPP−**2a** complex (vide supra).

The fluorescence lifetimes were also determined in CH_3CN and in CH_2Cl_2. The fluorescence lifetimes are summarized in Table 3. The fluorescence lifetime in each solvent is shortened only in the supramolecular complex (ZnTFPP−**2a**) as compared to the lifetime of ZnTFPP. The quenching rate constants (k_q) are determined from the fluorescence lifetimes (τ) in the presence of PyFc and the lifetime (τ_0) in the presence of pyridine using eq 4. The k_q values are also listed in Table 3.

$$k_q = \tau^{-1} - \tau_0^{-1} \quad (4)$$

To clarify the fluorescence quenching process of ZnTFPP by PyFc, the picosecond transient absorption spectra of the ZnTFPP−**2a** complex are measured in CH_3CN as shown in Figure S3a (Supporting Information). The picosecond transient absorption spectrum of ZnTFPP exhibits the S_1-S_n absorption spectrum at λ_{max} = 450 nm. When ZnTFPP forms the complex

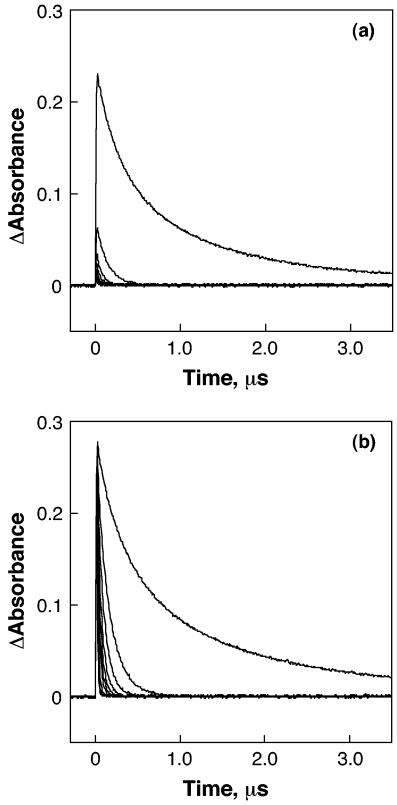

Figure 7. Decay dynamics of the triplet−triplet absorption due to ^{3}ZnTFPP* at 470 nm (a) in the ZnTFPP−**2a** complex and (b) in the ZnTFPP−pyridine complex in the presence of **2b** after laser excitation at 555 nm in deaerated benzene. [ZnTFPP] = 1.0×10^{-5} M, [**2a**] = $0-1.0 \times 10^{-3}$ M, [pyridine] = 2.1×10^{-2} M, [**2b**] = $0-1.1 \times 10^{-3}$ M.

with **2a** (1.0×10^{-2} M), the S_1-S_n absorbance disappears with the lifetime of 0.30 ns which agrees well with the fluorescence lifetime (vide supra). No T_1-T_n absorption appears, accompanied by disappearance of the S_1-S_n absorbance. This is in sharp contrast with the case of the ZnTFPP−pyridine complex which exhibits the conversion from the S_1 state to the triplet excited state (Figure S3b, Supporting Information).[38] Similar results were also obtained in benzene.

The photodynamics of the triplet excited state (^{3}ZnTFPP*) was also investigated by nanosecond laser flash photolysis in benzene and CH_3CN. The T_1-T_n absorbance of ZnTFPP decays obeying first-order kinetics. The addition of **2a** to a benzene solution of ZnTFPP results in a decrease in the initial T_1-T_n absorbance and the initial absorbance drop increases with increasing **2a** concentration as shown in Figure 7a. In addition, the triplet decay rate increases with increasing **2a** concentration (Figure 7a).

In contrast, no initial drop in absorbance due to ^{3}ZnTFPP* is observed in the case of the ZnTFPP−pyridine complex in the presence of **2b** which has no coordination site to ZnTFPP (Figure 7b). Such a difference between **2a** and **2b** is shown as plots of the initial drop in absorbance (ΔA) versus **2a** or **2b** concentration in Figure 8. This indicates that the complex formation of ZnTFPP with **2a** results in strong inhibition for the triplet generation and thus no singlet oxygen is formed (Figure 4).

The increase in the decay rate with increasing **2a** or **2b** is ascribed to the intermolecular quenching of the triplet excited state of ZnTFPP by **2a** or **2b**. The decay rate constant increases linearly with increasing **2a** or **2b** concentration. Such a linear

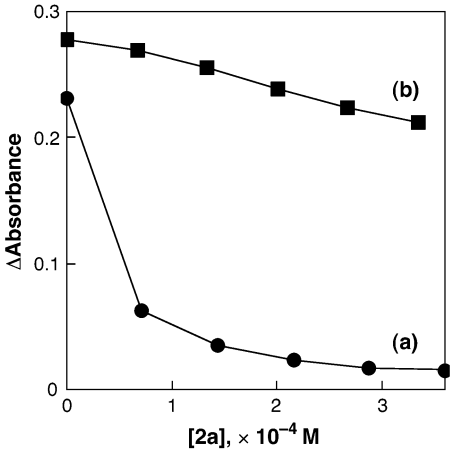

Figure 8. Plots of the initial absorbance vs [**2a**] for the triplet−triplet absorption due to ^{3}ZnTFPP* at 470 nm in (a) the ZnTFPP−**2a** complex and (b) the ZnTFPP−pyridine complex in the presence of **2b** after laser excitation at 555 nm in deaerated benzene.

SCHEME 2

(a) *Intra*molecular Photoinduced Electron Transfer (ZnTFPP–**2a** complex) in CH_3CN

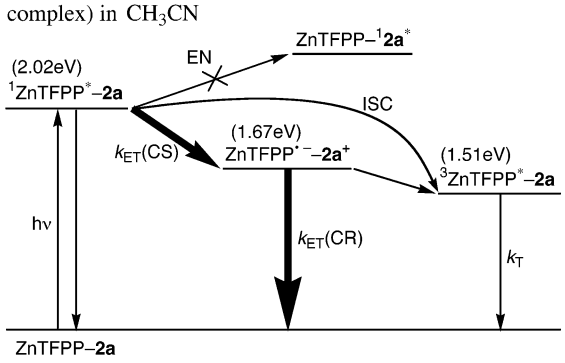

(b) *Inter*molecular Photoinduced Electron Transfer (ZnTFPP–pyridine complex + **2b**) in CH_3CN

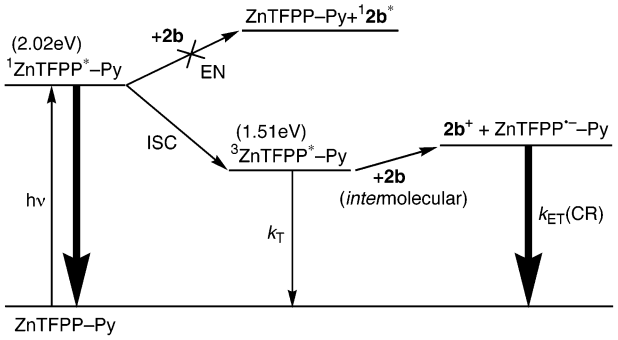

dependence of the decay rate constant on [**2a**] or [**2b**] confirms the bimolecular quenching of ^{3}ZnTFPP* by **2a** or **2b**. No new transient absorption band is observed, accompanied by decay of the triplet excited state. Similar results are obtained in CH_3CN (see Supporting Information S4 and S5).

Fluorescence Quenching Mechanism. The energy diagram of the ZnTFPP−**2a** complex is summarized in Scheme 2, where the energies were determined from the one-electron redox potentials (Table 1) and the singlet excited state energies obtained from the absorption and fluorescence maxima. The triplet excited energies were determined from the phosphorescence spectrum of ZnTFPP observed in deaerated frozen 2-methyltetrahydrofuran at 77 K.

Since the singlet excited state of ferrocene (2.46 eV)[39] is much higher in energy than the singlet excited state of ZnTFPP (2.02 eV), no singlet energy transfer from ^{1}ZnTFPP* to PyFc is expected to occur. In such a case, an intramolecular electron transfer from **2a** to ^{1}ZnTFPP* in the ZnTFPP−**2a** complex, which is energetically feasible, may be the only pathway for the fluorescence quenching (Scheme 2a). Such an electron transfer quenching of the singlet excited state porphyrin was reported for a carotenoid−porphyrin linked compound.[23] The formation of the charge-separated state formed by an electron transfer from the carotenoid to the singlet excited state porphyrin was confirmed by the characteristic transient absorption of the carotenoid radical cation.[23] In the case of ZnTFPP−**2a**, however, no transient absorption due to ZnTFPP$^{\bullet-}$ is observed, accompanied by the disappearance of the absorption due to ^{1}ZnTFPP* (Figure S3a, Supporting Information). No transient absorption due to ^{3}ZnTFPP* is observed at ^{3}ZnTFPP−**2a**, either (Figure S3a, Supporting Information). This indicates that the lifetime of the CS state is too short to be detected. The CS state decays at a much faster rate than the formation rate of the CS state, thus leading to regeneration of the ground state pair, ZnTFPP−**2a**, rather than to generation of the triplet excited state, ^{3}ZnTFPP*−**2a**, which is lower in energy than the CS state (Scheme 2a).[40]

The reason the back electron transfer to the ground state is much faster than to the triplet excited state is rationalized by a large reorganization energy involved in the back electron transfer, which may be comparable to the driving force of back electron transfer to the ground state (1.67 eV). In such a case, the back electron transfer to the ground state may be close to the Marcus top region[19] and thereby the back electron transfer rate to the ground state is much faster than the rate of electron transfer to the triplet excited state, which has a much smaller driving force (0.16 eV). The large reorganization energy required for the back electron transfer results from the significant change in the binding constant associated with the electron transfer reduction of ZnTFPP (vide supra). Upon photoinduced electron transfer in the ZnTFPP−**2a** complex, the binding between ZnTFPP$^{\bullet-}$ and **2a**$^+$ becomes smaller to facilitate the dissociation of the supramolecular complex. Such a dissociation process results in an increase in the distance between ZnTFPP$^{\bullet-}$ and **2a**$^+$, leading to the larger solvent organization associated with the back electron transfer. The larger reorganization energy of electron transfer at the larger distance between the donor and acceptor molecules has now been well-established.[7,41]

In fact, a large reorganization energy (1.41 eV) has recently been reported for electron transfer from the singlet excited state of zinc porphyrin to naphthalenediimide when they are linked with a relatively long spacer.[42] When naphthalenediimide is replaced by C_{60}, however, the reorganization energy of electron transfer becomes much smaller (0.59 eV) because of the intrinsic small reorganization energy of C_{60}. Although the CS state in the supramolecular system has rarely been detected,[16d] the CS state of a supramolecular triad system in which pyridine-linked C_{60} coordinates to zinc porphyrin has recently been detected by subpicosecond transient absorption spectral studies.[43] In this case, the small reorganization energy together with the stronger binding in the CS state enabled detection of the CS state. The CS state of a base-paired zinc porphyrin−dinitrobenzene supramolecular complex has also been detected by time-resolved electron paramagnetic resonance (EPR).[44] In contrast to such photoinduced oxidation of zinc porphyrin, the photoinduced reduction of zinc porphyrin by the ferrocene donor in the supramolecular complex in this study results in a weaker binding between the zinc porphyrin π radical anion and the nitrogenous base of the electron donor moiety, leading to the facile back electron transfer to the ground state. Such a finding was unprecedented since the present study is the first example of a supramolecular system of porphyrins in which porphyrins act as an electron acceptor.

The bimolecular quenching of the triplet excited state may also be caused by electron transfer from free **2a** (or **2b**) to ^{3}ZnTFPP* as shown in Scheme 2b. Although the CS state is higher in energy than ^{3}ZnTFPP*, the triplet excited state is quenched by **2a** or **2b** via the rate-determining electron transfer because of the much faster back electron transfer to the ground state than the triplet decay (Scheme 2b). In the case of bimolecular electron transfer reactions, a larger solvent reorganization energy at a large encounter distance is favorable to keep the rate constant large for a larger driving force, resulting in the lack of observation of the Marcus inverted region in the photoinduced bimolecular CS reactions.[41,45,46]

In conclusion, the supramolecular complex formation between ZnTFPP and **2a** provides a unique way to inhibit the singlet oxygen sensitization due to efficient intracomplex photoinduced electron transfer from **2a** to ^{1}ZnTFPP* and the facile back electron transfer from ZnTFPP$^{\bullet-}$ to **2a**$^+$ to the ground state rather than to the triplet excited state.

Acknowledgment. This work was partially supported by a Grant-in-Aid for Scientific Research Priority Area (13440216) and the Development of Innovative Technology (No. 12310) from the Ministry of Education, Culture, Sports, Science and Technology, Japan. H.I. thanks the Nagase Foundation for financial support.

Supporting Information Available: Synthetic procedure and characterization of **2b**, **3a**, and **3b** (S1 and S2) and the photodynamics of ^{1}ZnTFPP* in CH_3CN (S3) and ^{3}ZnTFPP* in CH_3CN (S4 and S5). This material is available free of charge via the Internet at http://pubs.acs.org.

References and Notes

(1) (a) Pandey, R. K.; Zheng, G. Porphyrins as Photosensitizers in Photodynamic Therapy. In *The Porphyrin Handbook*; Kadish, K. M., Smith, K. M., Guilard, R., Eds.; Academic Press: San Diego, 2000; Vol. 6, Chapter 43. (b) Bonnett, R. *Chem. Soc. Rev.* **1995**, *24*, 19. (c) Pandey, R. K.; Herman, C. *Chem. Ind.* (*London*) **1998**, 739.

(2) Dougherty, T. J.; Gomer, C.; Henderson, B. W.; Jori, G.; Kessel, D.; Korbelik, M.; Moan, J.; Peng, Q. *J. Natl. Cancer Inst.* **1998**, *90*, 889.

(3) Fukuzumi, S. In *The Porphyrin Handbook*; Kadish, K. M., Smith, K. M., Guilard, R., Eds.; Academic Press: San Diego, 2000; Vol. 8, pp 115−152.

(4) (a) *The Photosynthetic Reaction Center*; Deisenhofer, J., Norris, J. R., Eds.; Academic Press: San Diego, 1993. (b) *Anoxygenic Photosynthetic Bacteria*; Blankenship, R. E., Madigan, M. T., Bauer, C. E., Eds.; Kluwer Academic Publishing: Dordrecht, 1995.

(5) (a) Kurreck, H.; Huber, M. *Angew. Chem., Int. Ed. Engl.* **1995**, *34*, 849. (b) Harriman, A.; Sauvage, J.-P. *Chem. Soc. Rev.* **1996**, *26*, 41. (c) Wasielewski, M. R. *Chem. Rev.* **1992**, *92*, 435.

(6) (a) Gust, D.; Moore, T. A. In *The Porphyrin Handbook*; Kadish, K. M., Smith, K. M., Guilard, R., Eds.; Academic Press: San Diego, CA, 2000; Vol. 8, pp 153−190. (b) Gust, D.; Moore, T. A.; Moore, A. L. In *Electron Transfer in Chemistry*; Balzani, V., Ed.; Wiley-VCH: Weinheim, 2001; Vol. 3, pp 272−336. (c) Fukuzumi, S.; Imahori, H. In *Electron Transfer in Chemistry*; Balzani, V., Ed.; Wiley-VCH: Weinheim, 2001; Vol. 2, pp 927−975.

(7) (a) Imahori, H.; Tamaki, K.; Guldi, D. M.; Luo, C.; Fujitsuka, M.; Ito, O.; Sakata, Y.; Fukuzumi, S. *J. Am. Chem. Soc.* **2001**, *123*, 2607. (b) Fukuzumi, S.; Imahori, H.; Yamada, H.; El-Khouly, M. E.; Fujitsuka, M.; Ito, O.; Guldi, D. M. *J. Am. Chem. Soc.* **2001**, *123*, 2571. (c) Imahori, H.; Guldi, D. M.; Tamaki, K.; Yoshida, Y.; Luo, C.; Sakata, Y.; Fukuzumi, S. *J. Am. Chem. Soc.* **2001**, *123*, 6617.

(8) (a) Jensen, A. W.; Wilson, S. R.; Schuster, D. I. *Bioorg. Med. Chem.* **1996**, *4*, 767. (b) Wilson, S. R.; Schuster, D. I.; Nuber, B.; Meier, M. S.; Maggini, M.; Prato, M.; Taylor, R. *Fullerenes*; Kadish, K. M., Ruoff, R.

S., Eds.; John Wiley & Sons: New York, 2000; Chapter 3, pp 91−176. (c) Imahori, H.; Sakata, Y. *Eur. J. Org. Chem.* **1999**, 2445.

(9) (a) Osuka, A.; Mataga, N.; Okada, T. *Pure Appl. Chem.* **1997**, *69*, 797. (b) Sun, L.; Hammarström, L.; Åkermark, B.; Styring, S. *Chem. Soc. Rev.* **2001**, *30*, 36.

(10) (a) Hunter, C. A.; Sanders, J. K. M.; Beddard, G. S.; Evans, S. *Chem. Commun.* **1989**, 1765. (b) Anderson, H. L.; Hunter, C. A.; Sanders, J. K. M. *J. Chem. Soc., Chem. Commun*. **1989**, 226.

(11) (a) Lehn, J.-M. *Supramolecular Chemistry*: *Concepts and Perspectives*; VCH: Weinheim, 1995. (b) Sessler, J. L.; Wang, B.; Springs, S. L.; Brown, C. T. In *Comprehensive Supramolecular Chemistry*; Atwood, J. L., Davies, J. E. D., Eds.; Pergamon: New York, 1996. (c) Chang, C. J.; Brown, J. D. K.; Chang, M. C. Y.; Baker, E. A.; Nocera, D. G. In *Electron Transfer in Chemistry*; Balzani, V., Ed.; Wiley-VCH: Weinheim, 2001; Vol. 3, pp 409−461.

(12) (a) de Rege, P. J. F.; Williams, S. A.; Therien, M. J. *Science* **1995**, *269*, 1409. (b) Harriman, A.; Magda, D. J.; Sessler, J. L. *Chem. Commun.* **1991**, 345. (c) Sessler, J. L.; Wang, B.; Harriman, A. *J. Am. Chem. Soc.* **1995**, *117*, 704. (d) Berman, A.; Izraeli, E. S.; Levanon, H.; Wang, B.; Sessler, J. L. *J. Am. Chem. Soc.* **1995**, *117*, 8252.

(13) (a) Hayashi, T.; Ogoshi, H. *Chem. Soc. Rev.* **1997**, *26*, 355. (b) Blanco, M.-J.; Jiménez, M. C.; Chambron, J.-C.; Heitz, V.; Linke, M.; Sauvage, J.-P. *Chem. Soc. Rev.* **1999**, *28*, 293. (c) Willner, I.; Kaganer, E.; Joselevich, E.; Dürr, H.; David, E.; Günter, M. J.; Johnston, M. R. *Coord. Chem. Rev.* **1998**, *171*, 261.

(14) (a) D'Souza, F.; Rath, N. P.; Deviprasad, G. R.; Zandler, M. E. *Chem. Commun.* **2001**, 267. (b) D'Souza, F.; Deviprasad, G. R.; El-Khouly, M. E.; Fujitsuka, M.; Ito, O. *J. Am. Chem. Soc.* **2001**, *123*, 5277. (c) D'Souza, F.; Deviprasad, G. R.; Rahman, M. S. *Inorg. Chem.* **1999**, *38*, 2157. (d) D'Souza, F.; Zandler, M. E.; Smith, D. M.; Deviprasad, G. R.; Arkady, K.; Fujitsuka, M.; Ito, O. *J. Phys. Chem. A* **2002**, *106*, 649.

(15) (a) Da Ros, T.; Prato, M.; Guldi, D. M.; Ruzzi, M.; Pasimeni, L. *Chem.*−*Eur. J*. **2001**, *7*, 816. (b) Armaroli, N.; Diederich, F.; Echegoyen, L.; Habicher, T.; Flamigni, L.; Marconi, G.; Nierengarten, J.-F. *New J. Chem*. **1999**, 77. (c) D'Souza, F. *J. Am. Chem. Soc.* **1996**, *118*, 923.

(16) (a) Otsuki, J.; Harada, K.; Toyama, K.; Hirose, Y.; Araki, K.; Seno, M.; Takatera, K.; Watanabe, T. *Chem. Commun*. **1998**, 1515. (b) Imahori, H.; Yoshizawa, E.; Yamada, K.; Hagiwara, K.; Okada, T.; Sakata, Y. *Chem. Commun.* **1995**, 1133. (c) Imahori, H.; Yamada, K.; Yoshizawa, E.; Hagiwara, K.; Okada, T.; Sakata, Y. *J. Porphyrins Phthalocyanines* **1997**, *1*, 55. (d) Yamada, K.; Imahori, H.; Yoshizawa, E.; Gosztola, D.; Wasielewski, M. R.; Sakata, Y. *Chem. Lett.* **1999**, 235.

(17) Fukuzumi, S.; Ohkubo, K.; Imahori, H.; Shao, J.; Ou, Z.; Zheng, G.; Chen, Y.; Pandey, R. K.; Fujitsuka, M.; Ito, O.; Kadish, K. M. *J. Am. Chem. Soc*. **2001**, *123*, 10676.

(18) Imahori, H.; El-Khouly, M. E.; Fujitsuka, M.; Ito, O.; Sakata, Y.; Fukuzumi, S. *J. Phys. Chem. A* **2001**, *105*, 325.

(19) (a) Marcus, R. A.; Sutin, N. *Biochim. Biophys. Acta* **1985**, *811*, 265. (b) Marcus, R. A. *Angew. Chem., Int. Ed. Engl.* **1993**, *32*, 1111.

(20) (a) Davidson, R. S.; Trethewey, K. R. *Nature* **1977**, *267*, 373. (b) Demmig-Adams, B. *Biochim. Biophys. Acta* **1990**, *1020*, 1.

(21) Griffiths, M.; Sistrom, W. R.; Cohen-Bazire, G.; Stanier, R. Y. *Nature* **1955**, *176*, 1211.

(22) (a) Bensasson, R. V.; Land, E. J.; Moore, A. L.; Crouch, R. L.; Dirks, G.; Moore, T. A.; Gust, D. *Nature* **1981**, *290*, 329. (b) Moore, A. L.; Dirks, G.; Gust, D.; Moore, T. A. *Photochem. Photobiol.* **1980**, *32*, 691.

(23) Hermant, R. M.; Liddell, P. A.; Lin, S.; Alden, R. G.; Kang, H. K.; Moore, A. L.; Moore, T. A.; Gust, D. *J. Am. Chem. Soc.* **1993**, *115*, 2080.

(24) (a) Gust, D.; Moore, T. A.; Moore, A. L.; Jori, G.; Reddi, E. *Ann. N.Y. Acad. Sci.* **1993**, *691*, 32. (b) Nilsson, H.; Johansson, J.; Svanberg, K.; Svanberg, S.; Jori, G.; Reddi, E.; Segalla, A.; Gust, D.; Moore, A. L.; Moore, T. A. *Br. J. Cancer* **1994**, *70*, 873. (c) Reddi, E.; Segalla, A.; Jori, G.; Kerrigan, P. K.; Liddell, P. A.; Moore, A. L.; Moore, T. A.; Gust, D. *Br. J. Cancer* **1994**, *69*, 40. (d) Nilsson, H.; Johansson, J.; Svanberg, K.; Svanberg, S.; Jori, G.; Reddi, E.; Segalla, A.; Gust, D.; Moore, A. L.; Moore, T. A. *Br. J. Cancer* **1997**, *76*, 355.

(25) (a) Gurfinkel, M.; Thompson, A. B.; Ralston, W.; Troy, T. L.; Moore, A. L.; Moore, T. A.; Gust, D.; Tatman, D.; Reynolds, J. S.; Muggenburg, B.; Nikula, K.; Pandey, R.; Mayer, R. H.; Hawrysz, D. J.; Sevick-Muraca, E. M. *Photochem. Photobiol.* **2000**, *72*, 94. (b) van den Akker, J. T. H. M.; Speelman, O. C.; van Staveren, H. J.; Moore, A. L.; Moore, T. A.; Gust, D.; Star, W. M.; Sterenborg, H. J. C. M. *J. Photochem. Photobiol., B* **2000**, *54*, 108.

(26) Kadish, K. M.; Van Caemelbecke, E.; Royal, G. In *The Porphyrin Handbook*; Kadish, K. M., Smith, K. M., Guilard, R., Eds.; Academic Press: San Diego, 2000; Vol. 8, pp 1−114.

(27) Mann, C. K.; Barnes, K. K. *Electrochemical Reactions in Nonaqueous Systems*; Marcel Dekker: New York, 1990.

(28) Lindsey, J. S.; Wagner, R. W. *J. Org. Chem.* **1989**, *54*, 828.

(29) Lorkowski, H.-J.; Pannier, R.; Wende, A. *J. Prakt. Chem*. **1967**, *35*, 149.

(30) Kadish, K. M.; Shiue, L. R.; Rhodes, R. K.; Bottomley, L. A. *Inorg. Chem*. **1981**, *20*, 1274.

(31) Sanders, J. K. M.; Banpos, N.; Clude-Watson, Z.; Darling, S. L.; Hawaley, J. C.; Kim, H.-J.; Mak, C. C.; Webb, S. J. In *The Porphyrin Handbook*; Kadish, K. M., Smith, K. M., Guilard, R., Eds.; Academic Press: San Diego, 2000; Vol. 3, pp 1−48.

(32) Fukuzumi, S.; Kondo, Y.; Mochizuki, S.; Tanaka, T. *J. Chem. Soc., Perkin Trans. 2* **1989**, 1753.

(33) (a) Abraham, R. J.; Bedford, G. R.; McNeillie, D.; Write, B. *Org. Magn. Reson.* **1980**, *14*, 418. (b) Chachaty, C.; Gust, D.; Moore, T. A.; Nemeth, G. A.; Liddell, P. A.; Moore, A. L. *Org. Magn. Reson.* **1984**, *22*, 39.

(34) The limited solubility of **2a** and **3a** has precluded accurate determination of the K^- values in CH_3CN.

(35) Foote, C. S.; Clennan, E. L. Properties and Reactions of Singlet Oxygen. In *Active Oxygen in Chemistry*; Foote, C. S., Valentine, J. S., Greenberg, A., Liebman, J. F., Eds.; Chapman and Hall: New York, 1995; pp 105−140.

(36) Schmidt, R.; Afshari, E. *J. Phys. Chem.* **1990**, *94*, 8630.

(37) Under the present experimental conditions, 94% of ZnTFPP forms the complex with **2a**. There is a minor contribution from the intermolecular quenching of ^{3}ZnTFPP* by **2a** (see Figure 7).

(38) The absorption maximum of the triplet excited state (λ_{max} = 460 nm) is similar to that of the singlet excited state although the shape of the spectra are slightly different from each other.

(39) Sohn, Y. S.; Hendrickson, D. N.; Gray, H. B. *J. Am. Chem. Soc.* **1971**, *93*, 3603.

(40) The triplet energy determined at 77 K is assumed to be the same as the value at 298 K.

(41) (a) Gould, I. R.; Farid, S. *Acc. Chem. Res.* **1996**, *29*, 522. (b) Mataga, N.; Miyasaka, H. *Adv. Chem. Phys.* **1999**, *107*, 431.

(42) Imahori, H.; Yamada, H.; Guldi, D. M.; Endo, Y.; Shimomura, A.; Kundu, S.; Yamada, K.; Okada, T.; Sakata, Y.; Fukuzumi, S. *Angew. Chem., Int. Ed.* **2002**, *42*, 2344.

(43) D'Souza, F.; Deviprasad, G. R.; Zadler, M. E.; El-Khouly, M. E.; Fujitsuka, M.; Ito, O. *J. Phys. Chem. B* **2002**, *106*, 4952.

(44) (a) Berg, A.; Shuali, Z.; Asano-Someda, M.; Levanon, H.; Fuhs, M.; Mobius, K.; Wang, R.; Brown, C.; Sessler, J. L. *J. Am. Chem. Soc.* **1999**, *121*, 7433. (b) Asano-Someda, M.; Levanon, H.; Sessler, J. L.; Wang, R. *Mol. Phys.* **1998**, *95*, 935.

(45) (a) Rehm, A.; Weller, A. *Ber. Bunsen-Ges. Phys. Chem.* **1969**, *73*, 834. (b) Rehm, A.; Weller, A. *Isr. J. Chem.* **1970**, *8*, 259. (c) Bock, C. R.; Meyer, T. J.; Whitten, D. G. *J. Am. Chem. Soc.* **1975**, *97*, 2909. (d) Ballardini, R.; Varani, G.; Indelli, M. T.; Scandola, F.; Balzani, V. *J. Am. Chem. Soc.* **1978**, *100*, 7219.

(46) (a) Fukuzumi, S.; Kuroda, S.; Tanaka, T. *J. Am. Chem. Soc.* **1985**, *107*, 3020. (b) Fukuzumi, S.; Koumitsu, S.; Hironaka, K.; Tanaka, T. *J. Am. Chem. Soc.* **1987**, *109*, 305. (c) Fukuzumi, S.; Ohkubo, K.; Suenobu, T.; Kato, K.; Fujitsuka, M.; Ito, O. *J. Am. Chem. Soc.* **2001**, *123*, 8459.